Significance of cortactin as a prognostic factor in biliary cancer and its relevant signaling pathways as a therapeutic target

Yeona Cho

Department of Medicine

The Graduate School, Yonsei University

Significance of cortactin as a prognostic factor in biliary cancer and its relevant signaling pathways as a therapeutic target

Yeona Cho

Department of Medicine

The Graduate School, Yonsei University

Significance of cortactin as a prognostic factor in biliary cancer and its relevant signaling pathways as a therapeutic target

Directed by Professor Ik Jae Lee

The Doctoral Dissertation
submitted to the Department of Medicine,
the Graduate School of Yonsei University
in partial fulfillment of the requirements for the
degree of Doctor of Philosophy

Yeona Cho

December 2020

This certifies that the Doctoral Dissertation of Yeona Cho is approved.

Thesis Supervisor : Ik Jae Lee

Thesis Committee Member#1 : Hei-Cheul Jeung

Thesis Committee Member#2 : Joon Seong Park

Thesis Committee Member#3: Beom Jin Lim

Thesis Committee Member#4: Hee Chul Park

The Graduate School
Yonsei University

December 2020

ACKNOWLEDGEMENTS

I would like to extend immeasurable appreciation and deepest gratitude for many precious people's help and support. First of all, I would like to express my appreciation and great respect to my supervisor, Prof. Ik Jae Lee, for guiding me in every step of this thesis, research, and clinical practice. He has been a tremendous source of professional inspiration to me, as a great medical researcher as well as a radiation oncologist with enthusiasm and wisdom.

I would also like to show gratitude to the members of my advisory committee: Hei-Cheul Jeung, Joon Seong Park, Beom Jin Lim, and Hee Chul Park for their critical comments and valuable suggestions.

I express sincere thanks to Xiang Lan Zhang for her guidance in biomedical research. I also appreciate Ji Young Kim and You Keun Shin for their assistance in laboratory studies.

I really appreciate the instruction of the professors of the Department of Radiation Oncology of Yonsei University College of Medicine; Chang-Ok Suh, Jinsil Seong, Chang Geol Lee, Ki Chang Keum, Jaeho Cho, Yong Bae Kim, Woong Sub Koom, and Jun Won Kim. This thesis would not be possible without their excellent teaching and powerful interest in medical research. I also thank Jin Sung Kim, Hong In Yoon, Jee Suk Chang, and Kyung Hwan Kim, the young

committee member of Radiation Oncology Department. They always give me motivation and inspiration.

Lastly, I send my warmest regards to my family: my parents and my little sister. They always encouraged me, and provided unstinting support to allow me to strive to concentrate on my studies. I also send my deepest love to my daughter, Taein, and my husband, Ki Seok Kim.

For the rest of my life, I will dedicate my best effort to medical treatment and research for the patients with cancer.

<TABLE OF CONTENTS>

LIST OF FIGURES

LIST OF TABLES

ABSTRACT

Significance of cortactin as a prognostic factor in biliary cancer and its relevant signaling pathways as a therapeutic target

Yeona Cho

Department of Medicine
The Graduate School, Yonsei University

(Directed by Professor Ik Jae Lee)

Background and purpose: Biliary tract cancer has poor prognosis and high mortality, and its treatment options are often limited. Moreover, there is a lack of independent predictive factors for patient outcomes. Cortactin (CTTN), a primary substrate of the Src tyrosine kinase, has been implicated in cellular motility and invasion in various types of cancer. In this study, we explored the role of CTTN expression in biliary cancer in both in vitro and in vivo models. We also investigated CTTN expression in biliary cancer patients and its relationship with clinical factors and prognosis.

Methods and materials: We established a KKU-M213 biliary cancer cell line with CTTN and tyrosine466-phosphorylated CTTN (pY466-CTTN) double-knockdown. Cancer-associated fibroblasts (CAF) were obtained from a bile duct cancer patient. For the orthotopic models, tumor cells (1×10^7) were injected into the right liver area of 6- to 8-week-old female nude mice. In total, 116 patients with biliary cancer who underwent surgery between 2005 and 2013 were included, and their tissue microarrays were

constructed. The patients were divided into two groups according to their pY466-CTTN expression level: low CTTN (histoscore 0–100) and high CTTN (101–300).

Results: Upon co-culture with CTTN-knockdown cells, CAF invasion and proliferation were reduced. CTTN-knockdown KKU-M213 cell lines showed decreased invasion, mobility, mRNA expression level of CXCL10 and CCL2, and phosphorylation of MAPK pathway markers, namely p38, MEK, and ERK, compared with the scrambled control cells. Total EGFR levels continued to decrease even after EGF stimulation in CTTN-knockdown cells. However, in the scrambled control, the EGF-induced downregulation of the receptor was both delayed and impaired. In the mouse orthotopic tumor model, the CTTN expression was significantly associated with fibrosis around the tumor. Moreover, patients with higher expression of pY466-CTTN (n = 64) had significantly poorer disease-free survival (DFS) and overall survival (OS) (median DFS 7 vs. 16 months, p < 0.001; median OS 19 vs. 53 months, p < 0.001). According to Cox-regression multivariate analysis, high pY466-CTTN expression was a significant prognostic factor for DFS (HR, 2.33; 95% CI 1.52–3.57; p < 0.001) and OS (HR: 2.87; 95% CI: 1.78–4.61; p < 0.001). Desmoplasia and CAF infiltration were also more frequent in the CTTN high-expression group.

Conclusions: Our results showed that CTTN is significantly associated with the desmoplastic reaction, likely functioning by enhancing the invasion and proliferation of CAF. Patients with higher pY466-CTTN expression had poorer DFS and OS and increased desmoplasia around

tumors. The epidermal growth factor receptor (EGFR)–mitogen-activated protein kinases (MAPK) signaling pathway enhanced by CTTN might be associated with this signaling pathway. Further studies are needed to obtain a definitive conclusion of the signaling pathway.

Keywords: CTTN, cortactin, biliary cancer, cancer-associated fibroblast, desmoplasia, fibrosis

Significance of cortactin as a prognostic factor in biliary cancer and its relevant signaling pathways as a therapeutic target

Yeona Cho

Department of Medicine
The Graduate School, Yonsei University

(Directed by Professor Ik Jae Lee)

I. INTRODUCTION

Biliary tract carcinomas are rare, accounting for less than 1% of all cancers. However, their incidence has recently increased in Japan and industrialized countries, such as the USA. Particularly, in Korea, biliary tract carcinomas are common, ranking 9th in incidence and cancer mortality[1]. Its tumors have a poor prognosis and a high mortality, having a 5-year survival rate less than 30%, because they are usually detected late in the course of the disease. Their therapeutic treatment options are often limited. Although surgical treatment produces the best outcome, recurrences are frequent despite proper adjuvant therapy after surgery. Currently, the median survival is only approximately 12 months with a standard treatment using gemcitabine or 5-fluorouracil-based chemotherapy.

Recent studies have highlighted the importance of serum and molecular markers, including KRAS, TP53, and chromatin-remodeling, in the diagnosis and follow-up of biliary tract tumors. However, an independent predictive factor for

biliary cancer patients[2] and molecular markers that can be used as treatment targets are lacking.

Cortactin (*CTTN*), a major substrate of the Src tyrosine kinase, is a protein encoded by *CTTN* that is localized on the chromosome band 11q13[3,4]. *CTTN* has been implicated in cell proliferation, motility, and invasion in various types of cancer[5,6], and its elevated expression has been linked to tumorigenesis. In addition, it correlates with poor clinical outcomes in breast cancer, head and neck squamous cell carcinoma, hepatocellular carcinoma, colorectal adenocarcinoma, and melanoma[7-11]. Cortactin promoted cell motility and tumor metastasis by binding and activating the actin-related protein (Arp) 2/3 complex to regulate the formation of invadopodia[12]. In addition, its overexpression has been shown to enhance cell adhesion and form lamellipodium, which contribute to lamellipodial persistence and migration phenotypes[13]. However, the clinical significance and the underlying role of *CTTN* in the progression of biliary cancer remain unexplored.

In addition, the precise regulation of cortactin in the dynamic actin cytoskeleton should be clarified. The phosphorylation of tyrosine(Y) and serine/threonine in response to extracellular signals likely plays a role in cortactin regulation[14]. Y- 421 is the first identified phosphorylated amino acid residue that stabiliz´s the Src–cortactin complex, thus facilitating the subsequent phosphorylation of Y-466 and -482 [15].

In this study, we explored the role of *CTTN* expression in biliary cancer using both in vitro and in vivo models. Furthermore, we investigated the relationship of *CTTN* expression with the clinical factors and prognosis of patients with biliary cancer.

II. MATERIALS AND METHODS

1. Cell culture

Human cholangiocarcinoma cell lines MMNK1, KKU-M055, KKU-M213, and HUCCT1 were obtained from the Japanese Collection of Research Bioresources Cell Bank (Osaka, Japan). SNU245, SNU478, SNU869, SNU1079, and SNU1196 were supplied by the Korean Cell Line Bank (Seoul, Korea). Cells were subcultured at 80% confluence and maintained at 37 ℃ in a humidified incubator with 5% CO_2 and grown in DMEM (Lonza, Walkersville, Md, USA) and RPMI media (Lonza).

Fibroblast cell lines from the common bile duct cancer were gifted by Prof. Joon Seong Park. Patient-derived biliary tumor tissues were minced into sections of 1–3 mm in size and trypsinized for 30 min. Then, they werewashed in DMEM and plated in a petri dish with DMEM. Fibroblasts were allowed to grow out of tumor fragments for 2–3 weeks.

All media were supplemented with 10% (v/v) fetal bovine serum (SERANA). Cells were regularly examined for mycoplasma contamination.

2. Generation of CTTN-knockdown cells

CTTN shRNA was used for lentiviral transduction (ORIGENE TR30001, 5′-CACAAGCTGGAGTACAACTACAACAGCCA-3′). Scrambled control cells (Non-targeting) used scrambled sequence cassette (5′-GCACTACCAGAGCTAACTCAGATAGTACT-3′) into pGFP-C-shLenti. KKU-M213 cells were plated by 2×10^5 cells per 96-well, 24 hours before transduction. After the treatment of the lentiviral stock, the viral cell particle was incubated at 37 ℃ wovernight. Viral particle-containing medium was removed and replaced with a culture medium. Viral infection efficiency was assessed by determining the percentage of GFP-positive cells. For the selection

of stable knockdown clones, puromycin treatment was treated to kill untransduced cells. Harvested cells were plated to 3 plates (6 wells), and then treated with puromycin (2μg/mL). Knockdown of CTTN and Y466-phosphorylated CTTN (pY466-CTTN) was confirmed using western blot analysis. The clones with the most decreased expression of both CTTN and pY466-CTTN were selected and used for further evaluation.

3. Clonogenic assay

10,000cells/well of KKU-M213 wild-type and negative control and CTTN cells were seeded in 6 well plates. After 24 hours, cell counting was started. Then, cells were trypsinized to generate single cells, and the numbers of cells were counted by using CountessII automated cell counter (Thermo). This procedure was performed for 7 days every 24 hr, and data were analyzed.

4. Western blot analysis

Cell lysates were prepared in CMRC lysis buffer (50 mM Tris-HCl (pH 7.4), 150 mM NaCl, 1% Triton X-100, 1 mM EDTA, 1 mM EGTA, 10% glycerol, 5 mM NaF) on ice for 20 min. Lysates were collected, and supernatant was obtained by centrifugation at 12,500rpm, 4 ℃ for 15 min. Protein concentrations were measured by BCA assay (Thermo Fisher Scientific). 20 μg of proteins were mixed with 4X protein sample buffer (Bio-rad, add β-mercaptoethanol). The mixtures were boiled at 95 ℃ for 5 min. Proteins were separated on 10% sodium dodecyl sulfate-polyacrylamide gel electrophoresis (SDS-PAGE) and transferred to 0.45 μm PVDF membrane (Millipore). Membranes were treated with 5% skim milk in TBST (1M Tris-Cl (pH 8.0), Sodium Chloride (NaCl), TWEEN20) or 5% Bovine Serum Albumin in TBST for 2 hours at room temperature. Then, antibodies were added with 5% Bovine Serum Albumin in TBST at 4 ℃ overnight. Cortactin (Cell Signaling), phosphor-Cortactin (Biorbyt), Actin (Santa

Cruz) were used as detecting proteins. After washing 5 times with TBST, secondary antibody was blotted for 2 hours at room temperature. Chemiluminescence of proteins transferred to PVDF membranes was detected with ECL solution (visual protein).

5. Invasion assay

Matrigel-coated Transwell chambers (8 μm pore size, Corning) were used to analyze cell invasion. Lower chamber was filled with 700 μl culture media (RPMI with 10% FBS). After that, 1×106 cells in 200 μl of serum-free media were placed in the upper chamber. After incubation for 24 hours, fixation and staining solutions (Sysmex corporation) were used according to the manufacturer's instruction, and invading cells were counted. Photographs were taken at three spots after setting a certain standard. Then, cells were counted and averaged to draw a graph.

6. Wound-healing assay

Cell migration was confirmed by the wound-healing assay. Culture inserts (ibidi) for the wound-healing assays were used. Cells (2×10^5 cells in 100 μl) were seeded into each well. After cells reached a confluence of 95% in each well, culture insert was removed, and wells were filled with culture media. Degree of the wound closed was measured and photographed at every hour using an inverted microscope (ZEISS). The distance between the cell and cell was calculated based on the scale bar. 3 lines of constant distance were drawn. Each distance was calculated and averaged to draw a graph.

7. Co-culture for CAF proliferation analysis

Tissue Culture Treated Polystyrene Plates (0.4 μm pore size, Corning)

were used to co-culture. Lower chamber was filled with 50,000cells/well of Cancer associate fibroblast (DMEM with 1% FBS). After that, 500,000 cells/well KKU-M213 cell lines and scrambled control, experimental 2groups in serum-free media were placed in the upper chamber. After 24 hours, cell counting was started. Cells were trypsinized to generate single cells and counted using CountessII automated cell counter (Thermo). This procedure was performed for 3 days every 24hr. Then, data were analyzed.

8. Real-Time polymerase chain reaction (PCR)

KKU-M213 wild-type and negative control and shCTTN cells were seeded in a 100 mm plate. After 24 hours, RNA was isolated by using TRIZOL (MRC) reagent according to the manufacturer's protocol. With isolated RNA, cDNA was synthesized by using the RevertAid First StarandAce cDNA Synthesis kit (Thermo scientific) under the instruction from the manufacturer. Quantitative real-time PCR (qPCR) was performed with CFX Connect Real-Time PCR Detection System (Bio-Rad) and Power SYBR Green PCR Master Mix (Thermo Fishwe Scientific). Primer sequences using amplification of IL19, CXCL2, CXCL10, CXCL9, CCL2, and GAPDH were as follows:

Table 1. The primers of shRNA sequences.

Cytokines	Direction	Oligonucleotide Sequence 5'-3'
IL-19	Forward	5' – TCTACGTGGACAGGGTGTTC – 3'
	Reverse	5' – CTGACATTGCCGCAGAGTTT – 3'
CXCL2	Forward	5’ – AGTGTGAAGGTGAAGTCCCC – 3’
	Reverse	5' – TTCTTAACCATGGGCGATGC – 3'
CXCL10	Forward	5' – ACTGTACGCTGTACCTGCAT – 3'
	Reverse	5’ – GCAATGATCTCAACACGTGGA – 3’
CXCL9	Forward	5' – GTGAGAAAGGGTCGCTGTTC – 3'
	Reverse	5' – AATTTTCTCGCAGGAAGGGC– 3'
CCL2	Forward	5’ – GCAGCAAGTGTCCCAAAGAA – 3’
	Reverse	5' – TCGGAGTTTGGGTTTGCTTG – 3'
GAPDH	Forward	5' – AGGTCATCCCAGAGCTGAACG – 3'
	Reverse	5’ – CACCCTGTTGCTGTAGCCGTAT – 3’

PCR conditions were denaturated at 95℃ for 5 minutes, followed by 40 cycles of 95 ℃ for 10 s and 60 ℃ for 30 s were performed, and melting curves were obtained. All samples were processed in triplicate. GAPDH genes were used as housekeeping genes in this study. The 2–ΔΔCt method was used to determine the relative mRNA expression levels. The value of W + 0d was set as 1.

9. RNA microarray analysis

Data were summarized and normalized with the robust multi-average (RMA) method implemented in Affymetrix® Power Tools(APT). Results were concluded with gene-level RMA analysis and performed differentially expressed gene (DEG) analysis.

Statistical significance of the expression data was determined using fold change. For a DEG set, hierarchical cluster analysis was performed using

complete linkage and Euclidean distance as a measure of similarity.

Gene-Enrichment and Functional Annotation analysis for a significant probe list were performed using Gene Ontology (http://geneontology.org) and Kyoto Encyclopedia of Genes and Genomes (KEGG; http://kegg.jp). All data analysis and visualization of differentially expressed genes were conducted using R 3.3.3 (www.r-project.org).

10. Mouse orthotopic tumor model

Female, 6–8-week-old athymic nude (nu/nu) BALB/c mice were housed in laminar-flow cabinets under specific pathogen-free conditions. The present study was performed under protocols approved by the Animal Care and Use Committee of the College of Medicine of Yonsei University. AAALAC International accredits our animal research program.

For the orthotopic models, tumor cells (1×10^7) were injected into the right liver area of nude mice. Orthotopic mice were randomized into three treatment groups as follows (N=5 per group); scrambled shRNA group (implanted with KKU-M213 scrambled cells) as a control, and experimental two groups (implanted with KKU-M213 shCTTN#6 and shCTTN #17 cells). After 3 weeks, mice were sacrificed, and livers, including tumor, were removed.

11. Immunohistochemical staining

After deparaffinization with xylene and rehydration with graded alcohol, the tissue sections were incubated with a mixture of H_2O_2 and methanol at a dilution of 1:40 at room temperature for 10 min to block endogenous peroxidase activity. Antigen retrieval was performed with antigen retrieval buffer (Dako, Glostrup, Den- mark) using the pressure-cooking method. After blocking with 5% bovine serum albumin at room temperature for 5 min, sections were incubated with the primary antibody monoclonal rabbit anti-human cortactin IgG (#3503,

Cell Signaling Technology) at a dilution of 1:200 at room temperature for 2 h.

12. Patient selection

A total of 106 formalin-fixed, paraffin-embedded (FFPE) tumor specimens were obtained from patients with biliary tract cancer, excluding intrahepatic cholangiocarcinoma, who had been diagnosed at our institution, between 2006 and 2013. Tissue microarrays (TMA) were constructed using the FFPE specimens. Patient demographics included clinicopathological parameters such as age, gender, tumor location, TNM stage, and types of surgery. The clinical data of patients in this study were investigated retrospectively.

13. Statistical analysis

Mann-Whitney tests were employed to determine statistical significance as the non-parametric statistics. Cases were divided into two groups by the expression of pY466-CTTN (high vs. low). Fisher's exact test and Chi-square test were used to analyze potential association between the expression of CTTN and various clinicopathological parameters. Survival was estimated by the Kaplan-Meier method and evaluated by the log-rank test. Multivariate analyses of prognostic values were conducted using the Cox proportional hazards model. All analyses were carried out using the SPSS 23 for Windows (IBM, Armonk, NY, USA). A p-value of 0.05 was considered significant.

III. RESULTS

1. Expression of CTTN in biliary cancer cell lines

CTTN was expressed in most cell lines, and Y466-CTTN, its active form, was expressed in several cell lines (Figure 1A). Y421 was scarcely phosphorylated in biliary cell lines. Cell lines MMNK1, KKU-M213, SNU-869, and SNU-1079 expressed both CTTN and Y466-phosphorylated CTTN (pCTTN). Then, selection among the four types of cell lines was done to establish knockdown cell lines of both CTTN and Y466-phosphorylated CTTN (Figure 1B). For reproducible, long-term silencing of the target genes, short hairpin RNA (shRNA) of CTTN (shCTTN) using lentiviral particles was established. CTTN and pCTTN were successfully knocked down in KKU-M213 cells.

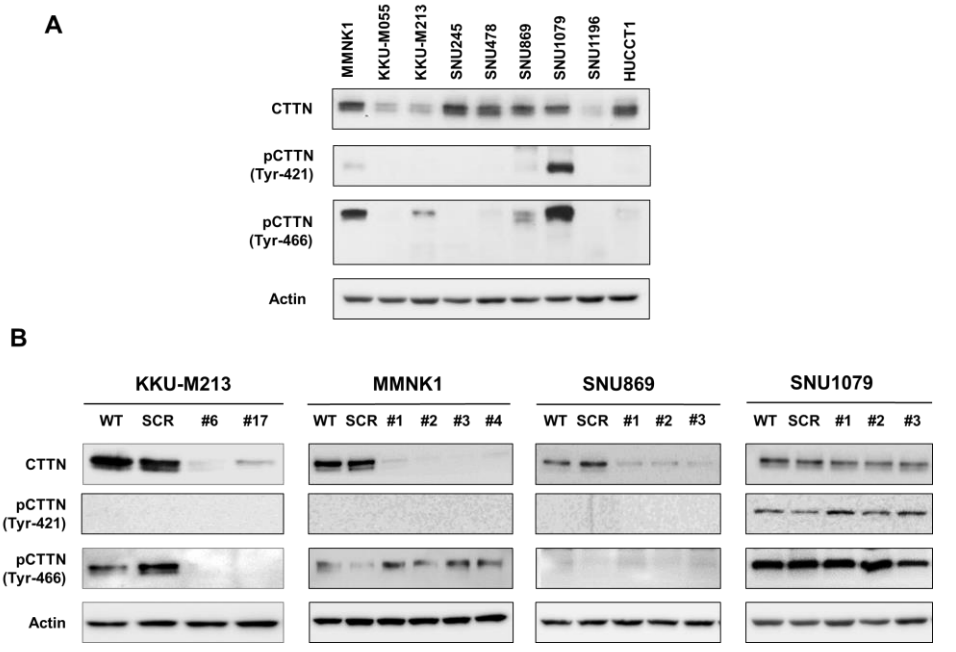

Fig. 1. Expression of CTTN in various biliary cancer cell lines and its knockdown. (A) Several biliary cancer cell lines showed increased expression of CTTN and tyrosin-phosphorylated CTTN. (B) Selection of four cell lines to establish CTTN-knockdown cells.

Two knockdown clones of KKU-M213, i.e., sh6 and sh17, were selected for subsequent analysis. Cell shape and cellular growth in a time-dependent manner were not significantly affected by the transfection of shCTTN in KKU-M213 cell lines (Fig. 2).

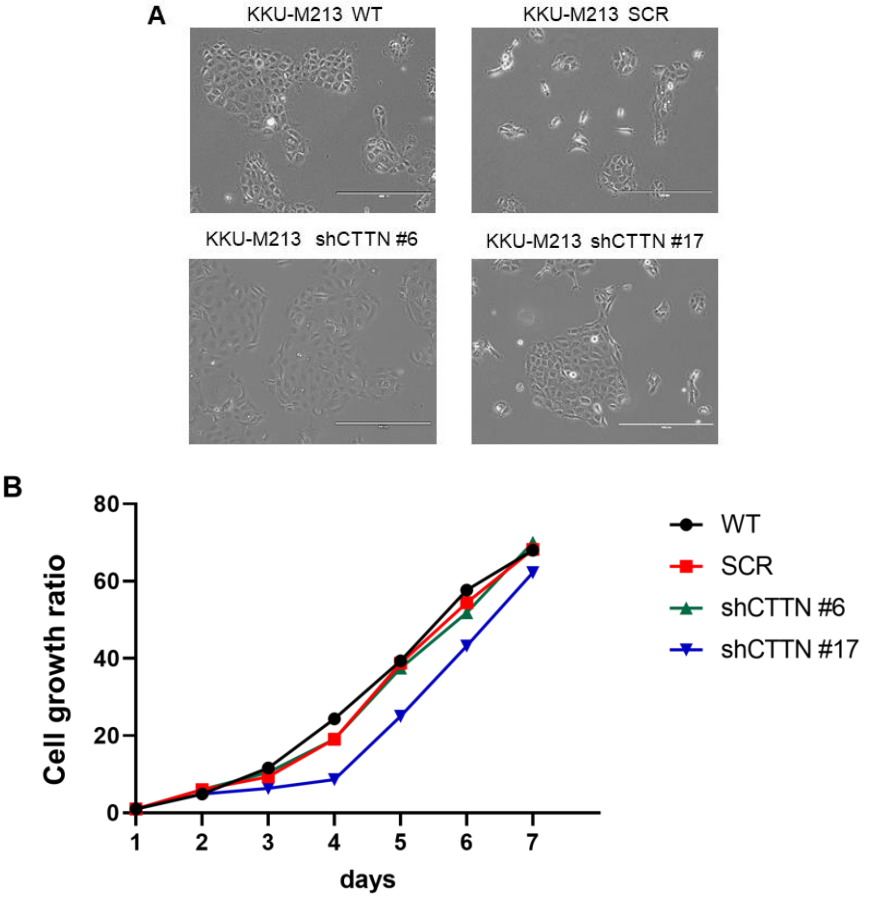

Fig. 2. The morphologic characteristics and cellular growth of KKU-M213 cells. (A) Size and shapes were not significantly different between the control and knockdown cells. (B) Cell growth assay was peformed for 7 days, and the number of cells was counted every 24 hours. CTTN knockdown did not affect the proliferation rates of KKU-M213 cells.

2. CTTN knockdown affects cellular invasion and migration

To investigate the role of CTTN in cellular invasiveness, invasion capability of KKU-M213 cells was measured. As shown in Figure 3, compared with control (scramble), transfection with shRNA #6 and shRNA #17 resulted in the reduction in the number of cells penetrating the Transwell membrane and Matrigel.

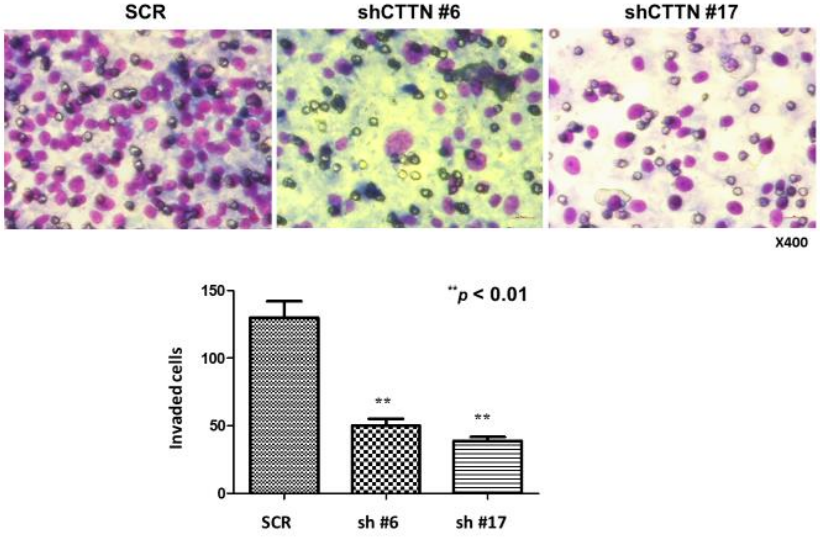

Fig 3. Transwell invasion assay of KKU-M213 cells. Invasion ability was significantly reduced in both CTTN-knockdown cell lines.

Wound-healing assays also showed that CTTN-knockdown cells migrated much more slowly than wild-type cells and scramble RNAi. Nine hours after wounding, the scrambled control cells reached confluence, whereas the CTTN-knockdown cells slowly migrated (Fig.4).

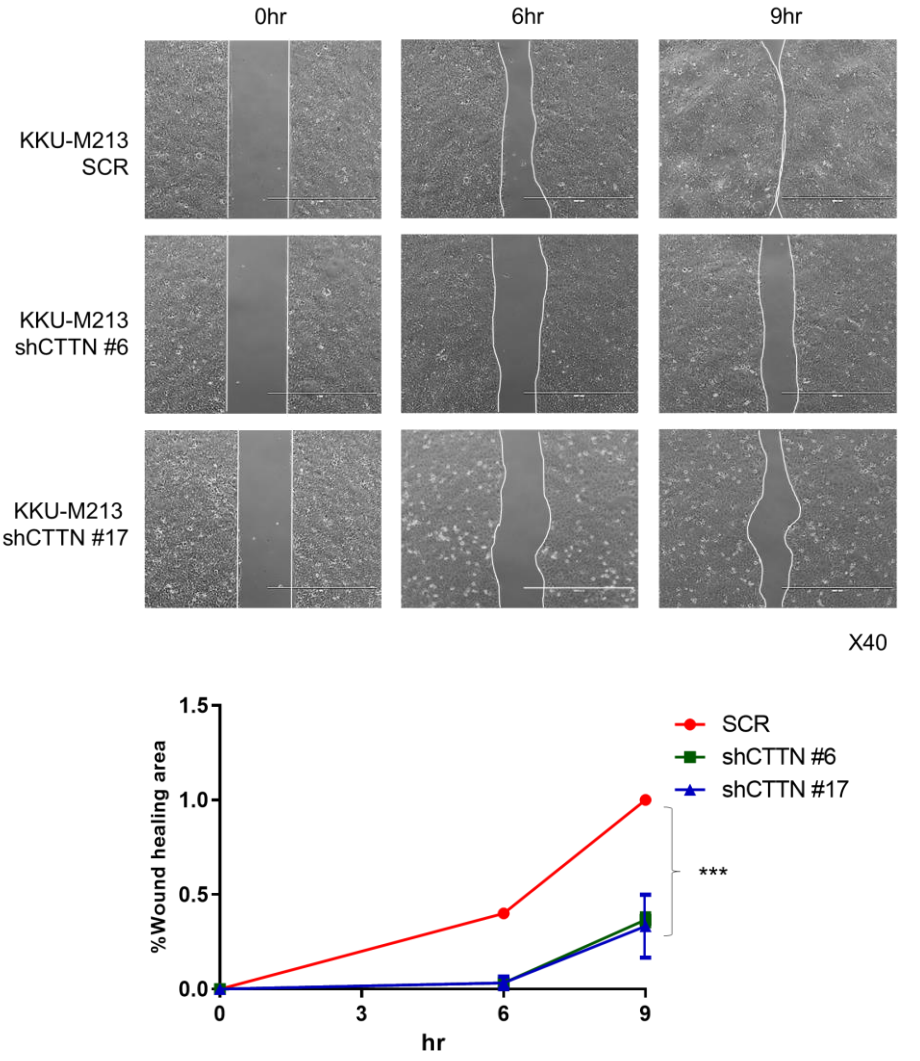

Fig. 4. Effect of CTTN on migration changes in KKU-M213 cells monitored using phase-contrast microscopy. Wound-healing assay was performed on KKU-M213 cells. The wound-healing area was measured by calculating the wound area in each period and is expressed as the percentage of the initial wound area at time zero compared with that in the scrambled control (*** $p < 0.001$)

3. CTTN promotes the invasion and proliferation of cancer-associated fibroblast

Cancer-associated fibroblasts (CAFs) from a common bile duct cancer patient were isolated and maintained in the FBS medium. The morphology of CAFs was elongated or stellated (Fig. 5A). Vimentin (fibroblast marker) and alpha-smooth muscle actin (α-SMA, a smooth muscle marker) using immunofluorescence were co-stained. Results indicated that most of the CAFs were double-positive for vimentin and α-SMA (Fig. 5B). Thus, CAFs were confirmed to be myofibroblasts, which is consistent with previous reports[16-18].

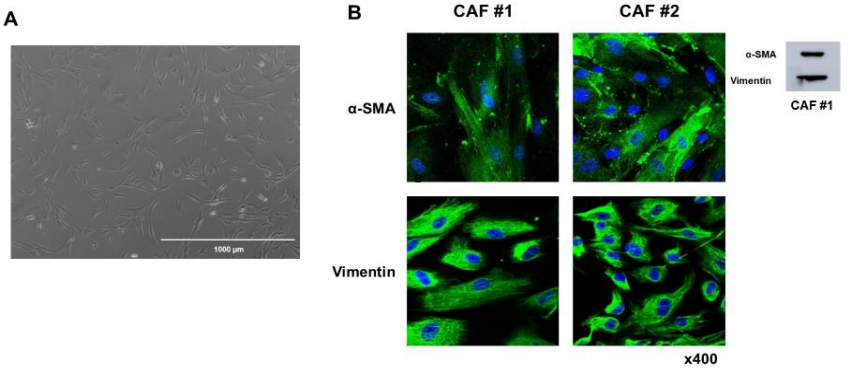

Fig. 5. Preparation of CAFs. (A) Characterization of CAFs isolated from a common bile duct cancer patient. Primary CAFs exhibited typical spindle-like mesenchymal morphology. Scale bar is 1000 μm. (B) Immunofluorescence staining of alpha-smooth muscle actin (α-SMA) and vimentin in CAFs. DAPI staining indicates cell nuclei (blue). Expression of α-SMA and vimentin in CAFs was also analyzed using western blot.

To detect the influence of CTTN on CAF invasion, an indirect co-culture model was adopted. Cells were processed for 48 hours, after which a Transwell assay was used to examine the invasion capability of CAF (Fig. 6A). CAF cells co-cultured with shCTTN cancer cells had fewer invaded cells than the cells co-cultured with WT/SCR KKU-M213 cells (Fig. 6B), indicating that CTTN is associated with the invasive ability of CAF cells.

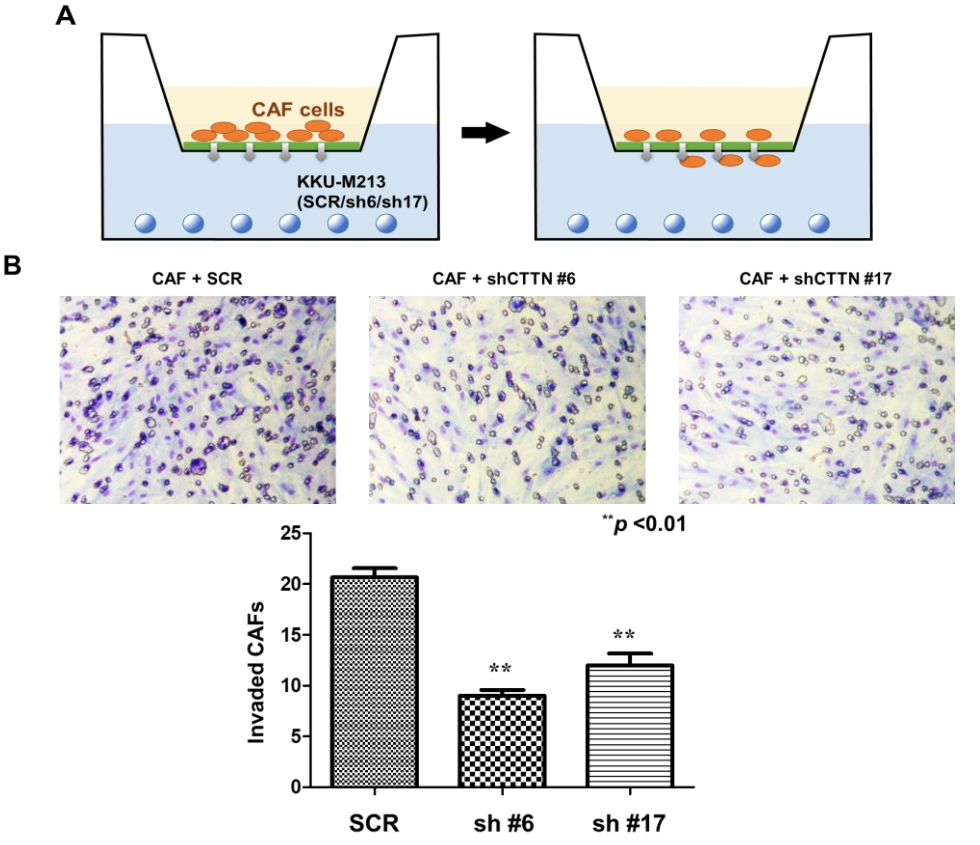

Fig 6. Upon the co-culture of CAF with KKU-M213 cancer cell lines, cortactin knockdown affected the invasion ability of CAF. (A) CAF cells of the Transwell penetrated the collagen membrane upon co-culture with KKU-M213 cells and finally attached to the lower surface of the Transwell. (B) Co-culture with CTTN-knockdown cells shows significantly decreased invasion ability of CAF.

A non-contact co-culture assay was also established to determine the influence of CTTN expression on CAF cell proliferation. Knockdown of CTTN decreased the proliferation of CAF cells (Fig. 7.)

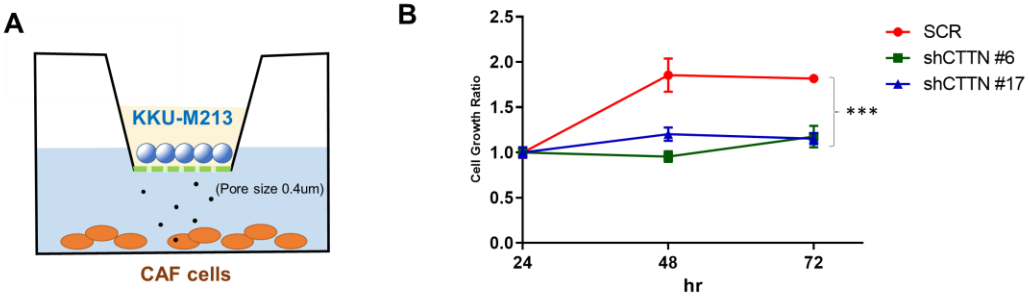

Fig. 7. Proliferation of CAF. (A) After a co-culture insert containing KKU-M213 cancer cells, (B) the proliferation of CAF cells affected by secreted cytokines was significantly suppressed by CTTN knockdown. (*** $p < 0.001$)

4. Cytokines CCL2 and CXCL10 and the related MAPK signaling pathway play a crucial role in the crosstalk between cancer cells and CAF

A. Distinctive expression profiles according to CTTN expression

mRNA expression profiles of wild-type, scrambled, CTTN knockdown KKU-M213 cell lines were prepared using oligonucleotide microarray. Global discrepancy in gene expression was checked according to the cortactin expression status using hierarchical clustering (Fig. 8A). Results, which demonstrated CTTN expression status, were discriminated well, indicating the possibility of selecting a group of genes associated with CTTN expression.

Consequently, mechanisms of the recruitment of CAF via cortactin

expression was proposed. Fig. 8B shows the KEGG pathway with significant differentially expressed genes related to signaling pathways or human diseases according to the CTTN expression status.

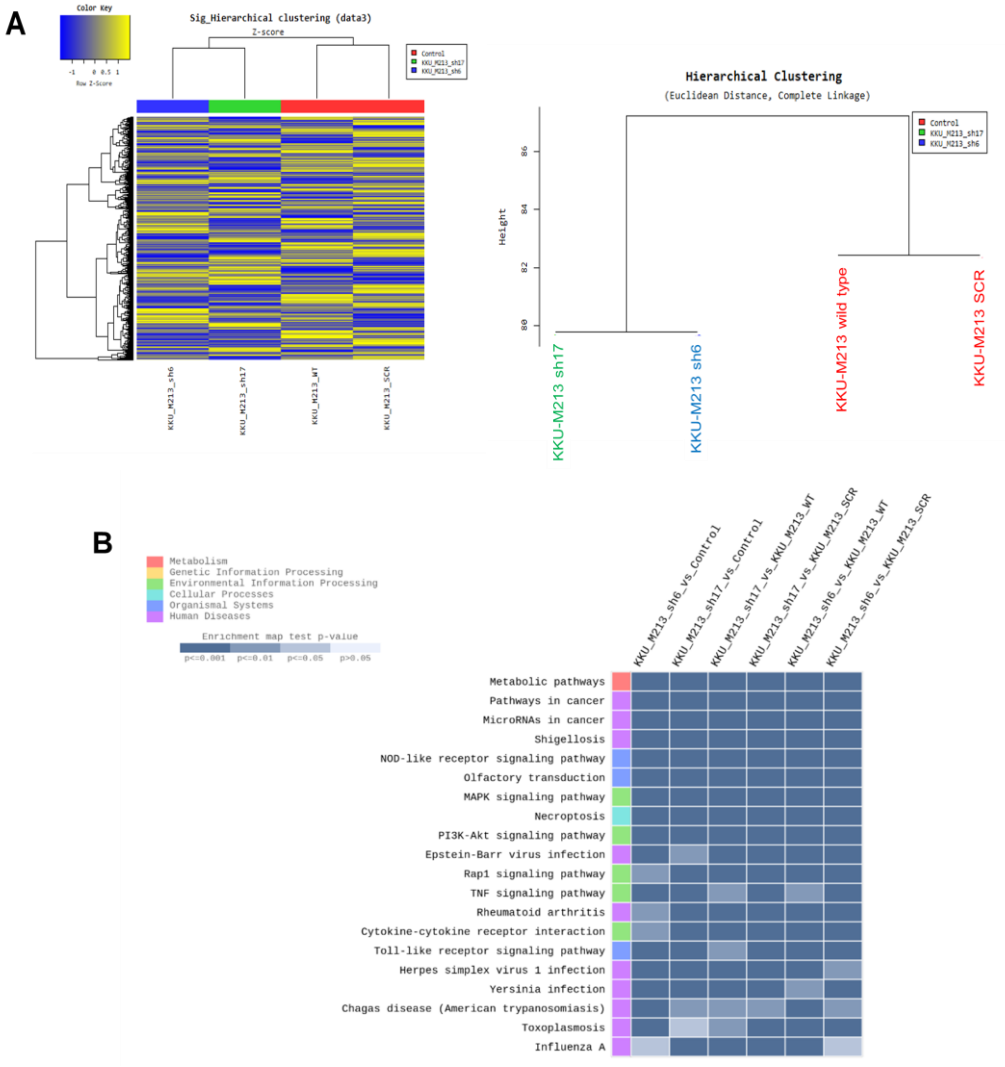

Fig 8. Supervised hierarchical clustering using the average linkage method.

(A) Patient samples were discriminated well by the cortactin expression status. Left side of the heat map represents CTTN knockdown, whereas the right shows the controls (wild-type and scrambled). (B) KEGG pathway analysis of the differentially expressed genes related to signaling pathways or human diseases.

B. Gene expression of several cytokines was decreased by CTTN knockdown.

Microarray confirmed the substantial downregulation of several cytokines, including IL19, CCL2, CXCL9, CXCR2, and CXCL10 (Fig. 9A) in CTTN-knockdown cells compared with that in the scrambled control. Real-time PCR was perfomed to validate the microarray data. The shRNA-mediated knockdown of CTTN attenuated the expression of IL19, CXCL9, CCL2, and CXCL10 (Fig. 9B).

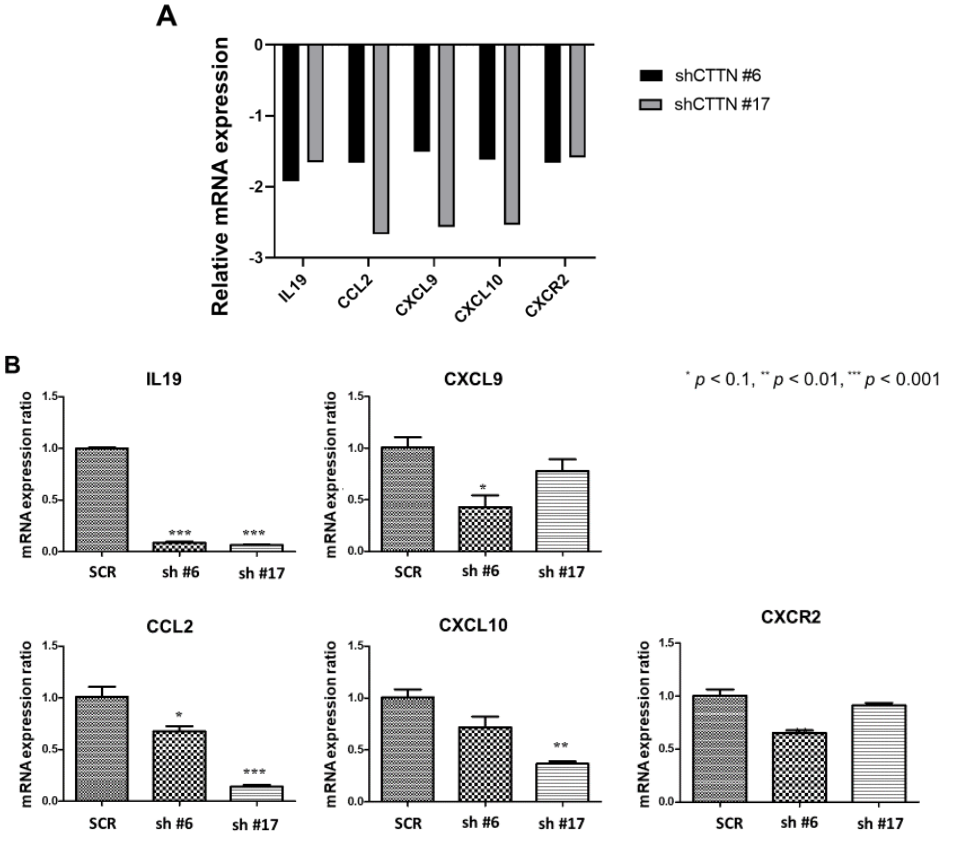

Fig. 9. Downregulation of several cytokines in CTTN-knockdown cell lines. (A) Microarray data show the significant fold-changes in gene expression. (B) Real-time PCR validated the microarray data.

C. Role of CXCL10 and CCL2 and its-related EGFR–MAPK signaling inactivation of CAF

The significantly downregulated cytokines, CXCL10, and CCL2, were the results of MAPK signaling pathways (Fig. 10A). As shown in Fig. 8B, the MAPK signaling pathway also significantly decreased based on the KEGG pathway analysis ($p < 0.001$). Therefore, knockdown of CTTN inhibited phosphorylation of ERK, MEK, and p38 (Fig. 10B). The MAPK pathway is often activated by the EGFR, and the EGFR expression was also reduced in shCTTN cell lines. Previous studies have revealed that cortactin overexpression inhibits ligand-induced downregulation of EGFR[19,20].

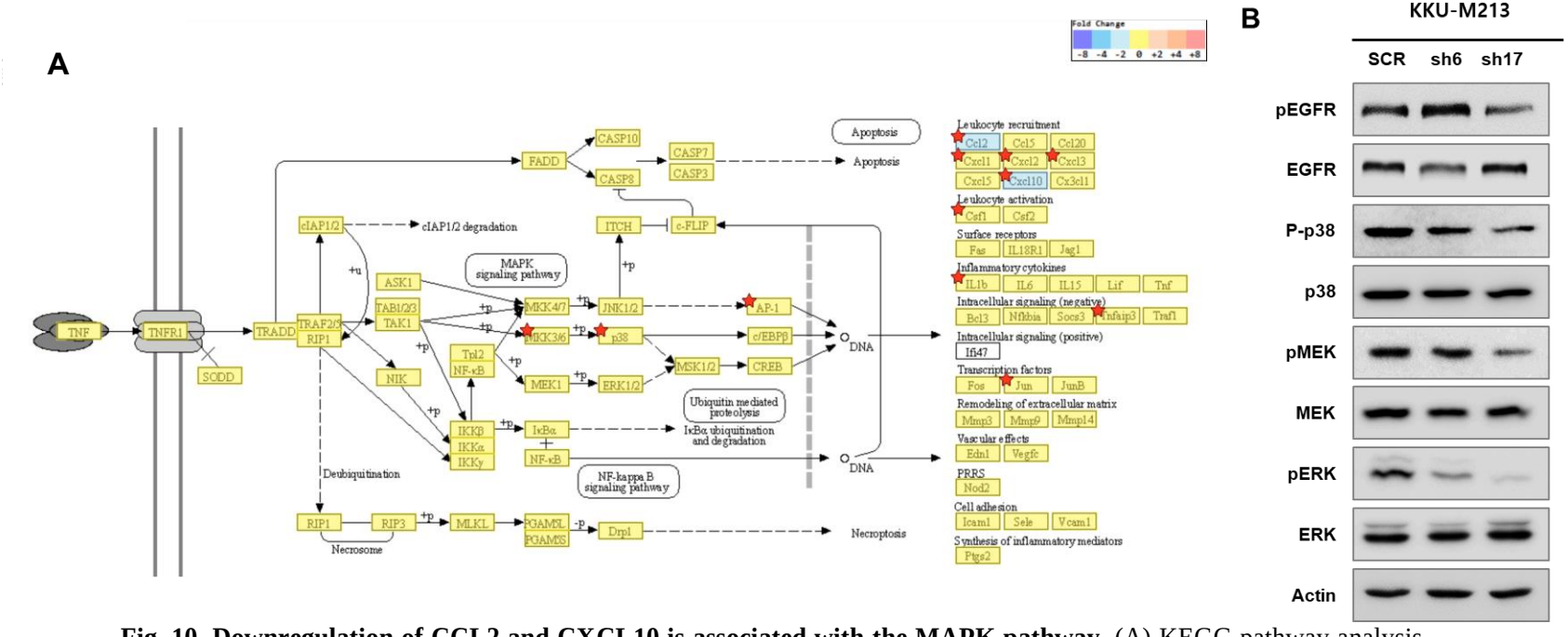

Fig. 10. Downregulation of CCL2 and CXCL10 is associated with the MAPK pathway. (A) KEGG pathway analysis of MAPK signaling. CCL2 and CXCL10 levels were significantly reduced in shCTTN cells (blue box). (B) Western blot analysis of p13 and MEK/ERK showed decreased phosphorylation in CTTN-knockdown cells.

To evaluate the effect on CAF proliferation and invasion, recombinant CCL2 and CXCL10 (R&D System, a Bio-Techne brand, MN, USA) were used. The invasion ability of CAF were significantly increased by CCL2 and CXCL10 levels (Fig.11A). In addition, the rate of cell proliferation in the presence of CXCL10 and CCL2 after 48 and 72 hours of culture was more significant than in the control (Fig. 11B).

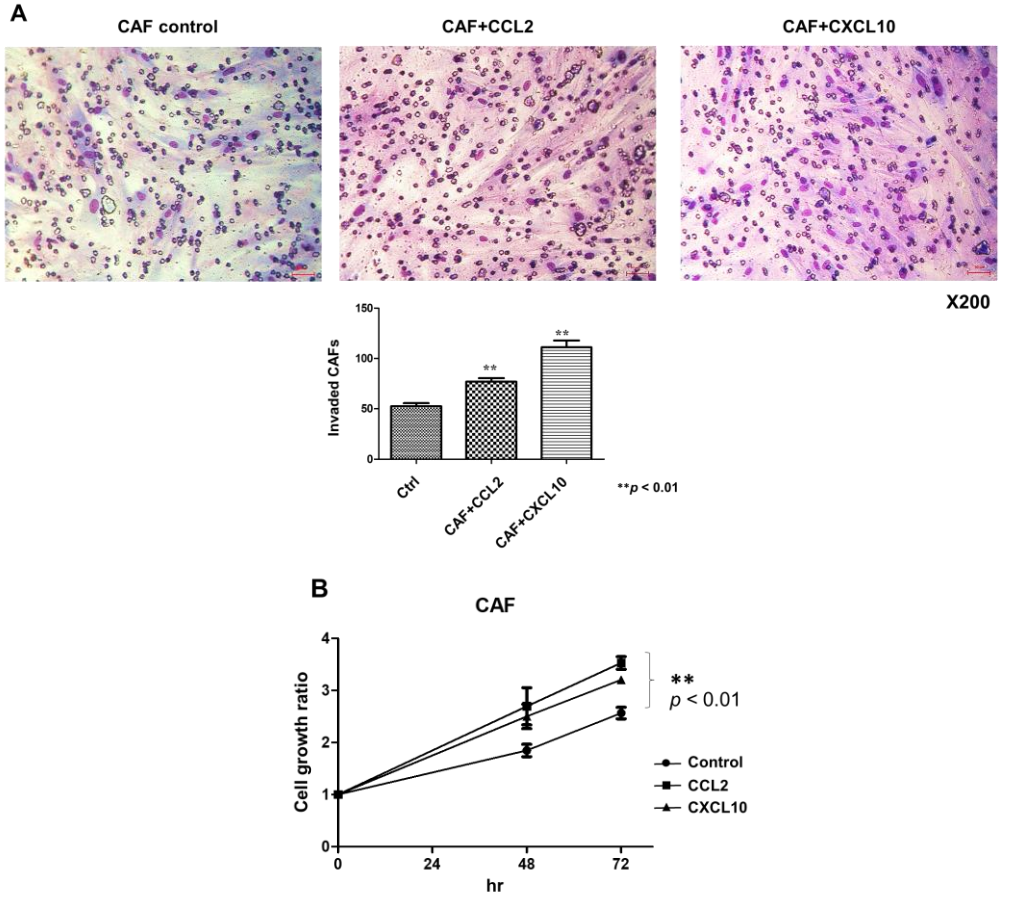

Fig. 11. Effect of CCL2 and CXCL10 on CAF activity . (A) Invasion ability of CAF was increased by the recombinant CCL2 and CXCL10. (B) Proliferation of CAF was also enhanced. (The concentration of the recombinant CCL2 and CXCL10 was 10 ng/ml and 0.3 ug/ml, respectively.)

D. CTTN inhibits EGFR degradation

Cells were subsequently serum-starved and then stimulated with EGF for 60 min. EGFR downregulation was determined by western blotting total cell lysates and quantitative analysis by densitometry provided a profile of ligand-induced receptor downregulation over time. (Fig 12.)

In shCTTN cells, total EGFR levels continuously decreased for 60 minutes after EGF treatment. However, in the scrambled control, the EGF-induced downregulation of the receptor was both delayed and impaired, resulting in sustained high expression of EGFR and pERK.

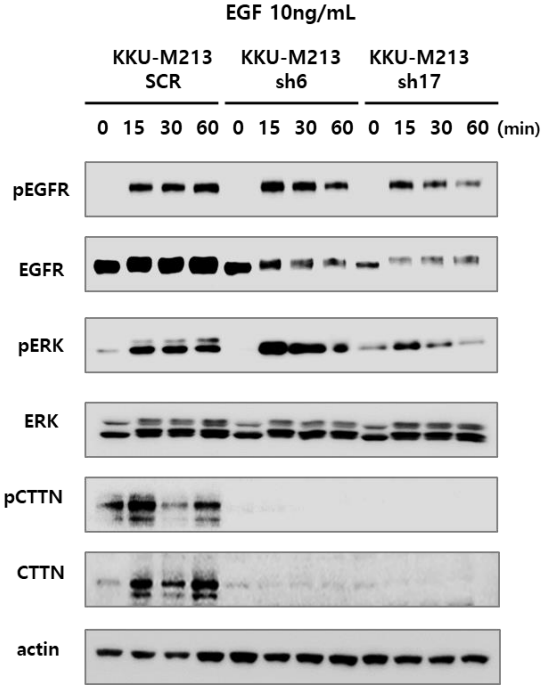

Fig. 12. CTTN inhibits ligand-induced EGFR downregulation. In the scrambled control, EGFR levels did not decrease, whereas in shCTTN cells, they were decreased.

5. CTTN is associated with desmoplasia in orthotopic model

Tumor was directly inoculated in the liver of the 5 mice of each group, and mice were euthanized three weeks later. Gross appearance of tumors and patterns of tumor growth showed no distinct difference (Fig.13A). The weight of the liver, including the tumor, was not significantly different among all groups (Fig. 13B).

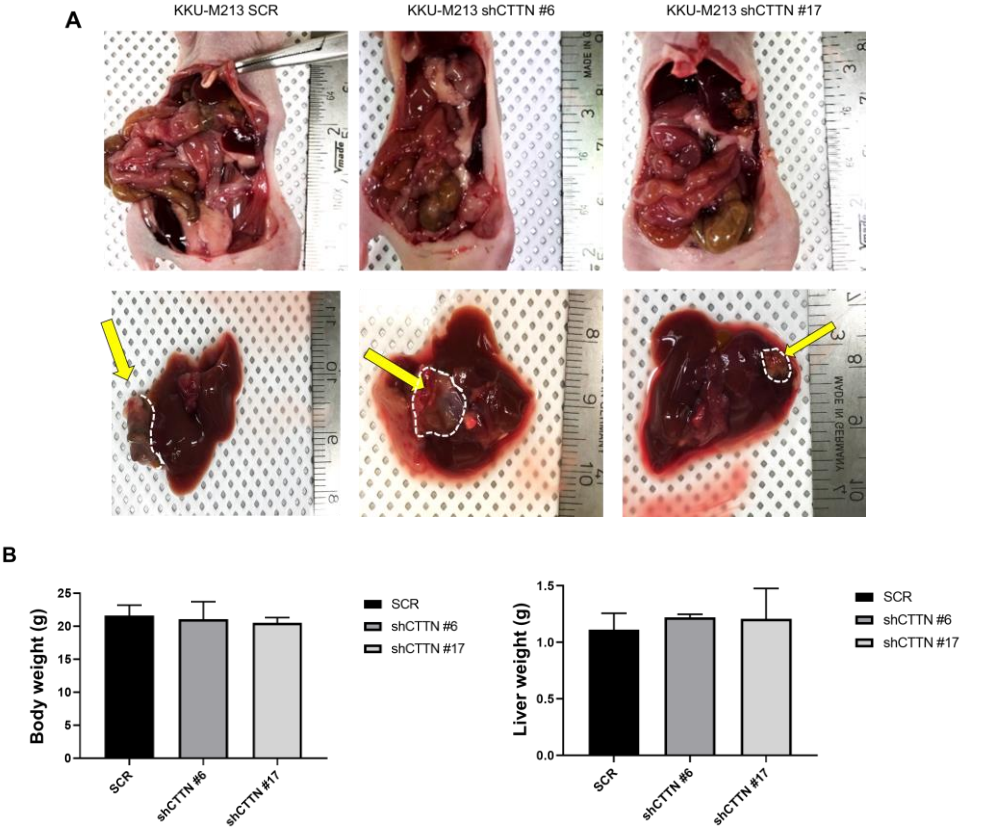

Fig. 13. Characterization of KKU-M213 tumor in the orthotopic model. (A) Representative gross tumor appearance and (B) the body and liver weights were not different among all groups.

KKU-M213 tumors and stroma are shown in Fig. 14A. Compared with the knockdown tumors, the shCTTN scrambled control had higher α-SMA expression, and the infiltration of α-SMA(+) CAF around the tumor was prominent. In the quantitative analysis, the relative α-SMA-positive area was markedly reduced in CTTN-knockdown tumors compared with that in the scrambled control (Fig. 14B).

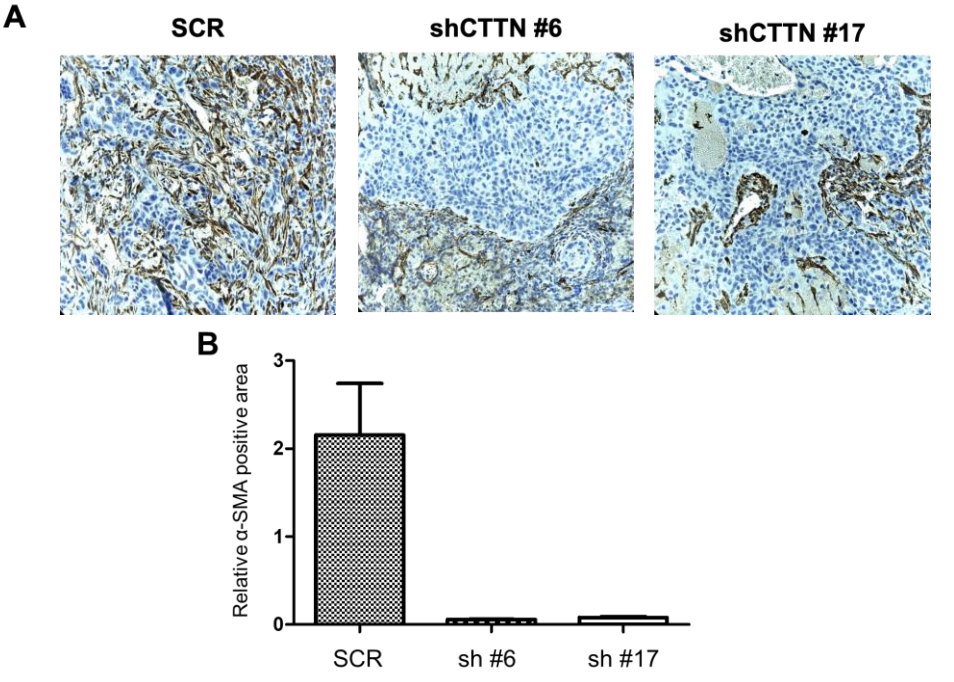

Fig. 14. Orthotopic tumor model reveals increased desmoplasia in the scrambled control. (A) α-SMA expression (brown) and the infiltration of α-SMA (+) CAF around tumors were significantly predominant in the shCTTN scrambled control. (B). Quantitative analysis shows marked reduction in the relative α-SMA-positive area in the CTTN-knockdown tumor ($p < 0.001$; Wilcoxon matched-pairs signed-rank test).

6. CTTN expression correlates with patient outcome

A. Patient characteristics

Patient characteristics, tumor type, and kind of treatment are summarized in Table 2. The median age was 68 years old (range, 45–86), and male patients were more common (59.5%). Common bile duct cancer was the most common type of cancer, accounting for 38.8%. The median value of carbohydrate antigen (CA) 19-9 and carcinoembryonic antigen (CEA) were 76.8 ng/ml (0.6–20160) and 2.4 ng/ml (0.3–1070), respectively. More than half of the patients (54.3%) received adjuvant treatment after primary surgery.

Most patients expressed CTTN (n = 108, 93.1%) and pY466-CTTN (n = 106, 91.4%). Meanwhile, pY421-CTTN was expressed in only 12 patients (10.3%) (Fig. 15A). A receiver operating characteristic (ROC) curve analysis was used to determine the cutoff points of the pY466- CTTN histoscore to discriminate patient prognosis. The cutoff value of histoscores is 100, with 71.9% sensitivity and 84% specificity (Area under curve = 0.76, $p < 0.001$) (Fig.15B). Patients were divided into two groups according to their pY466-CTTN expression level based on histoscore: 0–100 (CTTN low) and 101–300 (CTTN high)

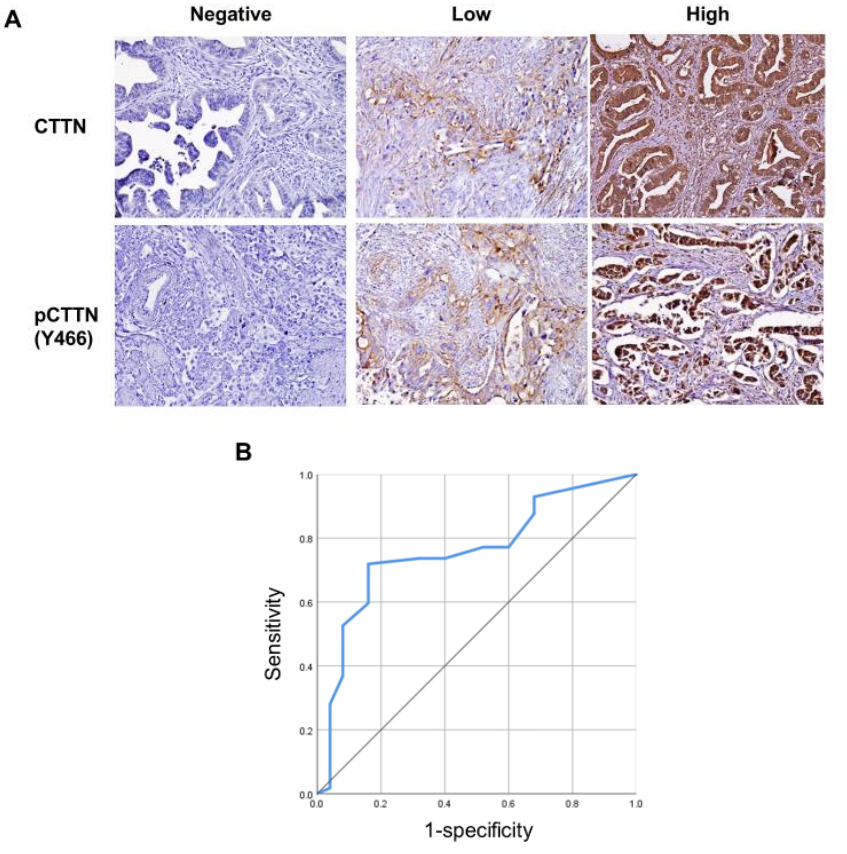

Fig. 15. Expression of CTTN and pY466-CTTN in patients with common bile duct cancer. (A) Histoscore (H-score) was calculated based on the percentage of CTTN positive cells and staining intensity. (B) ROC curve analysis revealed that the cutoff value of the H-score is 100, with 71.9% sensitivity and 84% specificity (Area under curve = 0.76, $p < 0.001$).

Patient age, sex, primary site, and stage were not different between the two groups. However, patients in the high CTTN group showed more frequent lymphovascular invasion (LVI; 48.4% vs. 28.8%, respectively; $p = 0.032$) and perineural invasion (PNI; 73.4% vs. 51.9%; $p = 0.016$). and had more poorly differentiated adenocarcinoma (29.7% vs. 17.3%; $p = 0.034$).

Table2. Patient characteristics

		Total n=116		CTTN low n=52		CTTN high n=64		*p*
Age	Median	68		67		69		0.364
	(range)	(45-86)		(45-81)		(57-86)		
Sex	Male	69	59.5	30	57.7	39	60.9	0.723
	Female	47	40.5	22	42.3	25	39.1	
Primary site	GB	20	17.2	9	17.3	11	17.2	0.473
	Hilar	29	25.0	11	21.2	18	28.1	
	CBD	45	38.8	24	46.2	21	32.8	
	AoV	22	19.0	8	15.4	14	21.9	
T stage	T1-2	63	54.3	31	59.6	32	50.0	0.301
	T3-4	53	45.7	21	40.4	32	50.0	
N stage	N0	64	55.2	29	55.8	35	54.7	0.907
	N1-2	52	44.8	23	44.2	29	45.3	
Grade	WD	15	12.9	11	21.2	4	6.3	0.034
	MD	73	62.9	32	61.5	41	64.1	
	PD	28	24.1	9	17.3	19	29.7	
CA19-9	Median	76.8		76.8		79.2		0.561
(ng/ml)	(range)	(0.6-20160)		(2.4-20160)		(0.6-14627.8)		
CEA	Median	2.4		2.2		2.5		0.477
(ng/ml)	(range)	(0.3-1070.0)		(0.3-1070.0)		(0.4-132.0)		
RM	(–)	90	77.6	40	76.9	50	78.1	0.877
	(+)	26	22.4	12	23.1	14	21.9	
LVI	(–)	70	60.3	37	71.2	33	51.6	0.032
	(+)	46	39.7	15	28.8	31	48.4	
PNI	(–)	40	34.5	24	46.2	16	25.0	0.016

	(+)	74	63.8	27	51.9	47	73.4	
Adj. Tx	None	53	45.7	23	44.2	30	46.9	0.839
	CTx	55	47.4	26	50.0	29	45.3	
	CRT	8	6.9	3	5.8	5	7.8	

Abbreviations: GB, gallbladder; CBD, common bile duct; AoV, ampulla of Vater; WD, well-differentiated; MD, moderately differentiated; PD, poorly differentiated; CA19-9, carbohydrate antigen 19-9; CEA, carcinoembryonic antigen; RM, resection margin; LVI, lymphovascular invasion; PNI, perineural invasion; Adj. Tx, adjuvant treatment; CTx, chemotherapy; CRT, chemoradiotherapy

B. Effect of CTTN on survival outcome

Among 116 patients, the median follow-up time was 23 months (2–66 months). The median DFS and overall survival (OS) of all patients were 10 and 25 months, respectively. Patients with higher CTTN expression had significantly poorer (DFS 7 months vs. 16 months; $p < 0.001$) and OS (19 months vs. 53 months; $p < 0.001$) (Fig. 16).

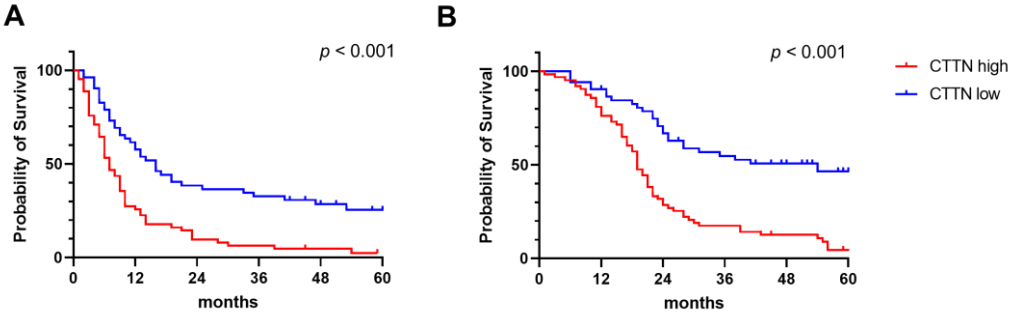

Fig. 16. Kaplan–Meir survival analysis for disease-free survival (A) and overall survival (B) according to CTTN expression.

According to the results of univariable analyses, advanced T and N stages, the presence of LVI, and high pY466-CTTN expression were significant predictors of poorer DFS ($p < 0.05$). Multivariable analysis results revealed that advanced T stage (hazard ratio [HR], 1.57; 95% confidence interval [CI], 1.05–2.35; $p = 0.03$), node metastasis (HR 1.52; 95% CI 1.01–2.3; $p = 0.046$), and high pY466-CTTN expression were significant predictors of poorer DFS (HR, 2.33; 95% CI 1.52–3.57; $p < 0.001$) (Table 3). Poor differentiation, the presence of LVI, and high CTTN expression were significant in univariate analysis for OS (Table 4). Multivariate analysis identified high pY466-CTTN expression as a significant prognostic factor for OS (HR 2.87; 95% CI 1.78–4.61; $p < 0.001$).

Table 3. Analysis of the factors associated with disease-free survival

	Univariable analysis		Multivariable analysis	
Variable	HR (95% CI)	*p*-value	HR (95% CI)	*p*-value
Age (> 65 vs. ≤ 65 years)	1.28 (0.85-1.92)	0.238		
Sex (female vs. male)	1.09 (0.73-1.62)	0.681		
T stage (T3-4 vs. T1-2)	1.63 (1.1-2.43)	0.016	1.60 (1.07-2.39)	0.022
N stage (N1-2 vs. N0)	1.66 (1.12-2.48)	0.012	1.57 (1.05-2.36)	0.027
Histologic grade (PD vs. others)	1.47 (0.94-2.3)	0.095		
CA19-9 (> 70 vs. ≤ 70 ng/ml)	0.86 (0.58-1.29)	0.471		
CEA (> 2.5 vs. ≤ 2.5 ng/ml)	1.06 (0.71-1.6)	0.765		
RM (positive vs. negative)	1.19 (0.75-1.9)	0.457		
LVI (yes vs. no)	1.66 (1.11-2.48)	0.013		
PNI (yes vs. no)	1.08 (0.71-1.64)	0.729		
CTTN expression (high vs.low)	1.02 (0.67-1.56)	0.924		
pY466- CTTN expression* (high vs. low)	2.44 (1.61-3.7)	<0.001	2.41 (1.59-3.65)	<0.001

Abbreviations: PD, poorly differentiated; CA19-9, carbohydrate antigen 19-9; CEA, carcinoembryonic antigen; RM, resection margin; LVI, lymphovascular invasion; PNI, perineural invasion. *CTTN and pY466-CTTN high expression > a histoscore of 100.

Table 4. Analysis of the factors associated with overall survival

	Univariable analysis		Multivariable analysis	
Variable	HR (95% CI)	*p*-value	HR (95% CI)	*p*-value
Age (> 65 vs. ≤ 65 years)	1.26 (0.82-1.95)	0.296		
Sex (female vs. male)	1.34 (0.87-2.05)	0.179		
T stage (T3-4 vs. T1-2)	1.47 (0.96-2.25)	0.073		
N stage (N1-2 vs. N0)	1.47 (0.96-2.24)	0.079		
Histologic grade (PD vs. others)	1.71 (1.06-2.77)	0.028	1.57 (0.97-2.54)	0.067
CA19-9 (> 70 vs. ≤ 70 ng/ml)	0.94 90.61-1.45)	0.786		
CEA (> 2.5 vs. ≤ 2.5 ng/ml)	1.16 (0.76-1.78)	0.5		
RM (positive vs. negative)	1.22 (0.74-2.01)	0.444		
LVI (yes vs. no)	1.91 (1.24-2.91)	0.003		
PNI (yes vs. no)	1.16 (0.74-1.84)	0.522		
CTTN expression* (high vs. low)	1.49 (0.67-2.41)	0.102		
pY466-CTTN expression* (high vs. low)	3.16 (1.98-5.04)	<0.001	3.08 (1.93-4.93)	<0.001

Abbreviations: PD, poorly differentiated; CA19-9, carbohydrate antigen 19-9; CEA, carcinoembryonic antigen; RM, resection margin; LVI, lymphovascular invasion; PNI, perineural invasion. *CTTN and pY466-CTTN high expression > a histoscore of 100.

C. CTTN is associated with higher CANF infiltration and increased desmoplastic reaction in patients with biliary cancer.

Higher CAF infiltration around the tumor was defined as an area of αSMA expression to be half of the tumor sample (Fig. 17A). In patients with biliary cancer, the high CTTN group showed higher αSMA expression than the low CTTN group (17B).

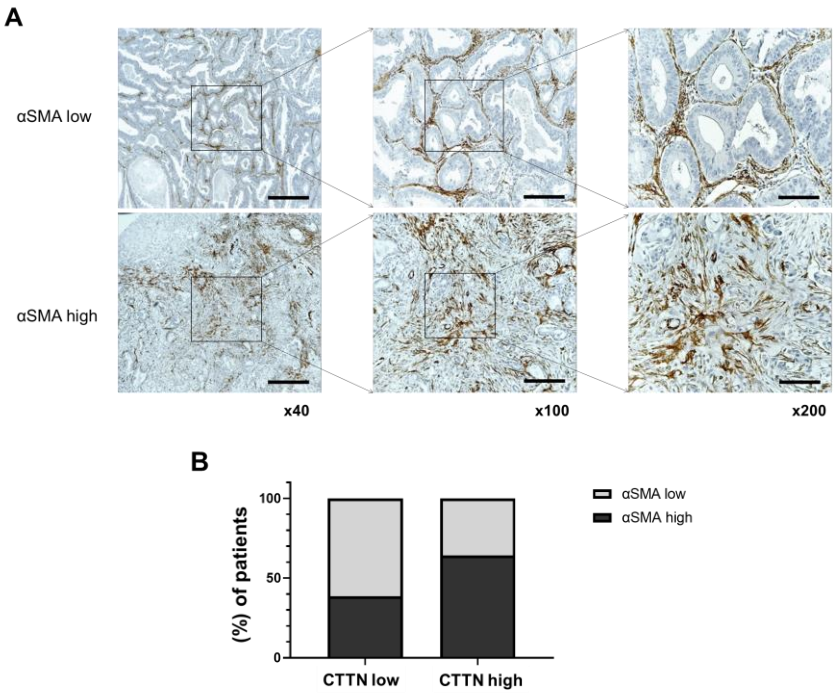

Fig. 17. CAF infiltration in patients with biliary cancer. Higher CAF infiltration around the tumor was defined as an area of αSMA expression to be half of the tumor sample (αSMA high). B. More patients in the high CTTN group showed higher CAF infiltration than the low CTTN group (62.5% vs. 40.4%, respectively; p = 0.018 by Pearson's Chi-square test).

Desmoplasia was defined as the presence of small tumoral nests surrounded by stromal fibrosis in at least one-third of the tumor sample (Fig. 18A). Desmoplasia in the TMA samples of each patient was classified as positive or negative by a pathologist. In the high CTTN group, 46 (71.9%) patients showed desmoplasia, whereas 42.3% (n = 22) in the low CTTN group had it (p = 0.001) (Fig. 18B).

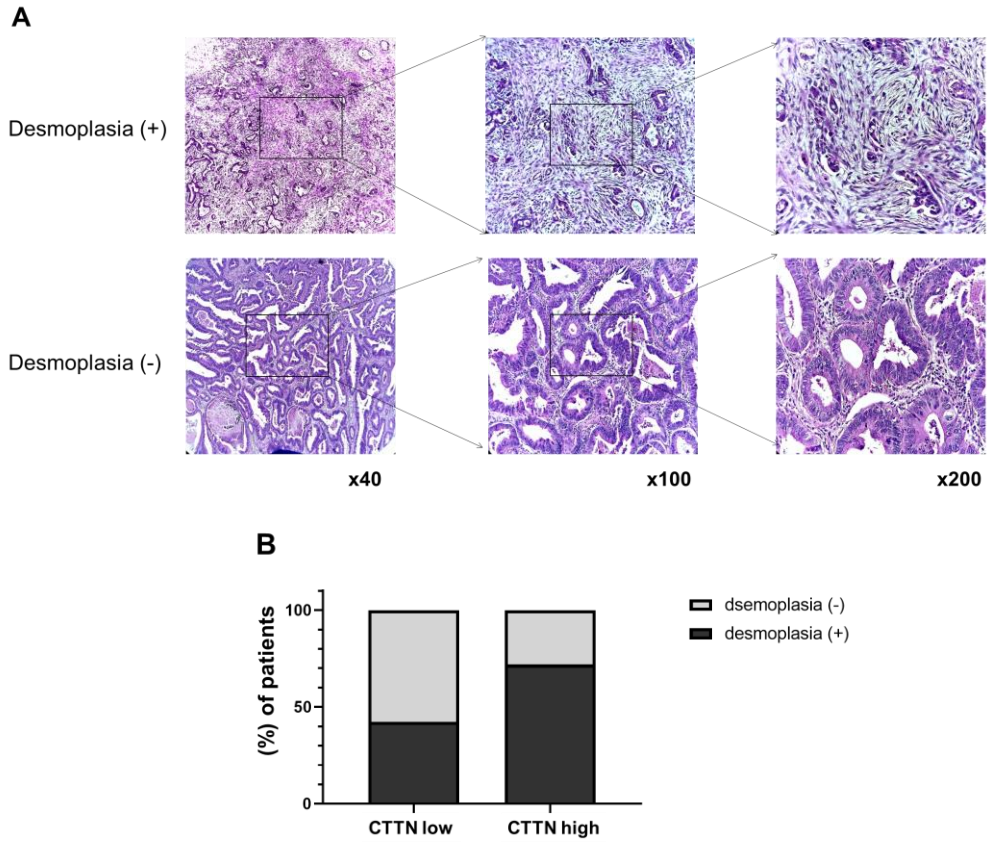

Fig. 18. Desmoplasia in patients with biliary cancer. (A) Desmoplasia (+) was defined as the presence of small tumoral nests surrounded by stromal fibrosis in at least one-third of the tumor sample. (B) More patients in the high CTTN group showed desmoplasia (71.9% vs. 42.3%, respectively; $p = 0.001$ by Pearson's Chi-square test).

IV. DISCUSSION

In this study, CTTN, especially pY466-CTTN, not only increased the invasion and migration of biliary cancer cells but also activated CAF to promote fibrosis and desmoplasia around the tumor. We speculate that CTTN promotes the secretion of cytokines, such as CCL2 and CXCL10, that eventually increases CAF recruitment and invasion CAF around the tumor. In particular, an activated EGFR–MAPK signaling pathway might be associated with this process (Fig. 19).

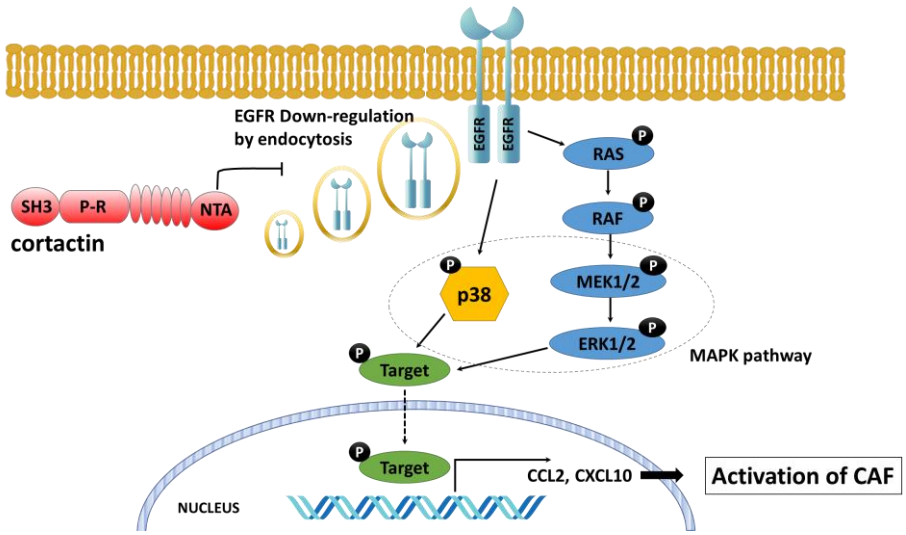

Fig. 19. Proposed role of cortactin in CAF activation. Cortactin inhibits the ligand-induced degradation of EGFR, resulting in sustained EGFR–MAPK pathway. As a consequence, the transcription of cytokines, such as CCL2 and CXCL10, is increased, and CAF are activated.

Cortactin is mainly involved in cell structure, such as the cytoskeleton, and cellular movement. Because cortactin proteins are located close to the cell membrane, several studies have focused on the function of cortactin as a signaling molecule. We also suggested whether cortactin crosstalk with the

tumor microenvironment, and we found that CTTN influenced the activity of CAF.

CAF activity eventually promotes desmoplasia around the tumor. In this study, we observed that the increased invasion of α-SMA (+) CAF in the orthopoic model, especially in the invasive head of the tumor. Stromal fibrosis was also prominent not only in the mouse orthotopic model but also in the patients' TMA analysis. Moreover, patients expressing pY466-CTTN had poor OS and DFS.

The desmoplastic tumor microenvironment is associated with poor prognosis, thus presenting a clinical challenge. Reactive tumor stroma and fibrogenic connective tissues are located around the tumor. Thus, chemoresistance could arise both biologically and physiologically[21]. The desmoplastic reaction, occurring within individual tumor cells, reduces the effectiveness of treatment via three different general types of mechanisms: first, development of target cell resistance to drug uptake; second, altered sensitivity of drug target sites in target sites through, for example, increased expression of anti-apoptotic proteins; and third, increased drug efflux from target cells, which prevents the drugs from reaching their intended site of action[22]. Additionally, the desmoplastic stroma could be a physiological barrier to drug absorption or penetration into target tissues due to poor tissue vasculature or perfusion. It also increases interstitial fluid pressure or induces the production of extracellular matrix (ECM) proteins[23].

CAF supports tumor progression through tissue scaffolding. Its role has been mainly studied in pancreatic cancer, wherein CAFs stimulate matrix stiffening through the remodeling of the ECM, a process mediated by expression of lysyl oxidases (LOX) and matrix metalloproteinases (MMPs) and the secretion of chemokines and growth factors, including TNFα and TGFβ[24]. In addtion, CAFs are involved in the maintenance of tumor metabolism, thus facilitating a state

of chemoresistance[25,26] In biliary cancers, α-SMA expression in fibroblasts is associated with poor prognosis [27,28]

Immunotherapy is one of the mainstream of cancer therapy recently; however, patient response to immunotherapy might be poor in patients with tumors with active desmoplasia[24]. The desmoplastic stroma of tumors could be a barrier to immune cell infiltration. Watt et al. have found that CD8+ T cells, CD20+ B cells, CD56+ NK cells, and FOXP3+ T regulatory cells (Treg cells) cannot infiltrate the juxta-tumoral stroma of cancer cells in pancreatic cancer[29]. Additionally, the desmoplastic reaction involves both the proliferation of fibroblasts and the deposition of multiple ECM components. Infiltrating immune cells and tumor cells also contribute to the fibrogenesis mediated by the pancreatic stellate cells (PSCs) via various signaling mechanisms, including those with the following primary signaling molecules: TGFβ, PDGF, and FGF2. These signaling molecules are secreted by tumor epithelial cells and infiltrating immune cells. Autocrine signaling of TGFβ mediated by PSCs also contribute to cell proliferation and increased ECM deposition[21].

Therefore, therapeutic approaches for reducing desmoplasia-induced chemoresistance are needed. However, there exist no drug that directly inhibit cortactin protein or *CTTN*. A previous study has found that pTyr421-cortactin is dephosphorylated by curcumin. Curcumin physically interacted with PTPN1 tyrosine phosphatases to increase its activity and lead to the dephosphorylation of pY421-cortactin[30]. However, because curcumin was effective only in some cell lines, further studies will be needed to validate its usefulmes in biliary cancer.

Furthermore, we suggest that the EGFR–MAPK pathway promoted by CTTN expression is involved in the activation of CAF. Timpsons et al. have reported that cortactin overexpression attenuated the ligand-induced downregulation of EGFR, leading to sustained signaling[19]. They also suggested

that cortactin overexpression is associated with resistance against the EGFR inhibitor, Gefitinib, in head and neck cancer patients[20]. Another study on colorectal cancer has suggested that the overexpression of *CTTN* suppresses the ubiquitin-mediated EGFR degradation induced by EGF, resulting sustained MAPK signaling by inhibiting the association between EGFR and c-Cbl[31].

In this study, the suppression of *CTTN* did not affect cancer cell growth. However, its downregulation has been shown to reduce colorectal cancer cell proliferation[31]. Its overexpression suppresses the ubiquitin-mediated EGFR degradation that is induced with EGF, leading to sustained MAPK signaling. In addition, *CTTN* has been associated with advanced stages of colorectal cancer. However, its proliferation effect on tumors is rarely reported. Other studies have revealed that *CTTN* is not associated with EGFR levels and do not have an effect on the proliferation of breast or hepatocellular cancer cells[8,10,32]. This might be due to the cellular specificity and mutations of the EGFR signaling pathway. In this study, the expression of *CTTN* did not increase cellular proliferation in both in vitro and in vivo models, and *CTTN* was not associated with advanced staging. However, the high CTTN group was associated with adverse features, such as poor differentiation, LVI, and PNI, indicating that *CTTN* expression may be associated with tumor aggressiveness. Whether *CTTN* expression promotes cancer cell growth should be explored by future studies.

There are several limitations to this study. Although we demonstrated that Y466 phosphorylation is required, it is insufficient to conclude that phosphorylation is crucial for activating the pathway that recruits CAF. After knockdown, the phosphorylated and de-phosphorylated clones were not completely separated in any cell lines. Therefore, the independent role of phosphorylation was not evaluated. However, most of the studies have indicated that phosphorylation is essential for activating CTTN, and pY466-CTTN was also significant in our results. Second, only one biliary cancer cell

line was evaluated, and a validation study with other cell lines is thus required. Third, although cellular proliferation activities could be associated with EGFR, we did not evaluate the EGFR mutation status of our patients as the KKU-M213 cell line does not harbor the said mutation. Nevertheless, our findings suggest the important role of CTTN in biliary cancer.

V. CONCLUSION

Our results showed that CTTN expression is significantly associated with increased desmoplastic reaction. The invasion and proliferation of CAF decreased in CTTN-knockdown cell lines. In addition, patients with higher expression of pY466-CTTN had poorer DFS and OS and increased desmoplasia around tumors. The EGFR–MAPK signaling pathway enhanced by CTTN might be associated with this process. Further studies are needed to elucidate the signaling pathway involved.

REFERENCES

1. Resistry KCC. Annual reports of cancer statistics in Korea 2017. 2017;11-1352000-000145-10.

2. Nakamura H, Arai Y, Totoki Y, Shirota T, Elzawahry A, Kato M, et al. Genomic spectra of biliary tract cancer. Nat Genet 2015;47:1003-10.

3. Kanner SB, Reynolds AB, Vines RR, Parsons JT. Monoclonal antibodies to individual tyrosine-phosphorylated protein substrates of oncogene-encoded tyrosine kinases. Proc Natl Acad Sci U S A 1990;87:3328-32.

4. Wu H, Reynolds AB, Kanner SB, Vines RR, Parsons JT. Identification and characterization of a novel cytoskeleton-associated pp60src substrate. Mol Cell Biol 1991;11:5113-24.

5. Weed SA, Parsons JT. Cortactin: coupling membrane dynamics to cortical actin assembly. Oncogene 2001;20:6418-34.

6. Daly RJ. Cortactin signalling and dynamic actin networks. Biochem J 2004;382:13-25.

7. Hirakawa H, Shibata K, Nakayama T. Localization of cortactin is associated with colorectal cancer development. Int J Oncol 2009;35:1271-6.

8. Chuma M, Sakamoto M, Yasuda J, Fujii G, Nakanishi K, Tsuchiya A, et al. Overexpression of cortactin is involved in motility and metastasis of hepatocellular carcinoma. J Hepatol 2004;41:629-36.

9. Eke I, Deuse Y, Hehlgans S, Gurtner K, Krause M, Baumann M, et al. beta(1)Integrin/FAK/cortactin signaling is essential for human head and neck cancer resistance to radiotherapy. J Clin Invest 2012;122:1529-40.

10. Li Y, Tondravi M, Liu J, Smith E, Haudenschild CC, Kaczmarek M, et al. Cortactin potentiates bone metastasis of breast cancer cells. Cancer Res 2001;61:6906-11.

11. Xu XZ, Garcia MV, Li TY, Khor LY, Gajapathy RS, Spittle C, et al. Cytoskeleton alterations in melanoma: aberrant expression of cortactin, an actin-binding adapter protein, correlates with melanocytic tumor progression. Mod Pathol 2010;23:187-96.

12. Weed SA, Karginov AV, Schafer DA, Weaver AM, Kinley AW, Cooper JA, et al. Cortactin localization to sites of actin assembly in lamellipodia requires interactions with F-actin and the Arp2/3 complex. J Cell Biol 2000;151:29-40.

13. Bryce NS, Clark ES, Leysath JL, Currie JD, Webb DJ, Weaver AM. Cortactin promotes cell motility by enhancing lamellipodial persistence. Curr Biol 2005;15:1276-85.

14. van Damme H, Brok H, Schuuring-Scholtes E, Schuuring E. The redistribution of cortactin into cell-matrix contact sites in human carcinoma cells with 11q13 amplification is associated with both overexpression and post-translational modification. J Biol Chem 1997;272:7374-80.

15. Huang C, Liu J, Haudenschild CC, Zhan X. The role of tyrosine phosphorylation of cortactin in the locomotion of endothelial cells. J Biol Chem 1998;273:25770-6.

16. Kalluri R, Zeisberg M. Fibroblasts in cancer. Nat Rev Cancer 2006;6:392-401.

17. Choe C, Shin YS, Kim C, Choi SJ, Lee J, Kim SY, et al. Crosstalk with cancer-associated fibroblasts induces resistance of non-small cell lung cancer cells to epidermal growth factor receptor tyrosine kinase inhibition. Onco Targets Ther 2015;8:3665-78.

18. Romero IL, Mukherjee A, Kenny HA, Litchfield LM, Lengyel E. Molecular pathways: trafficking of metabolic resources in the tumor microenvironment. Clin Cancer Res 2015;21:680-6.

19. Timpson P, Lynch DK, Schramek D, Walker F, Daly RJ. Cortactin overexpression inhibits ligand-induced down-regulation of the epidermal growth factor receptor. Cancer Res 2005;65:3273-80.

20. Timpson P, Wilson AS, Lehrbach GM, Sutherland RL, Musgrove EA, Daly RJ. Aberrant expression of cortactin in head and neck squamous cell carcinoma cells is associated with enhanced cell proliferation and resistance to the epidermal growth factor receptor inhibitor gefitinib. Cancer Res 2007;67:9304-14.

21. Whatcott CJ, Posner RG, Von Hoff DD, Han H. Desmoplasia and chemoresistance in pancreatic cancer. In: Grippo PJ, Munshi HG, editors. Pancreatic Cancer and Tumor Microenvironment. Trivandrum (India); 2012.

22. Szakacs G, Paterson JK, Ludwig JA, Booth-Genthe C, Gottesman MM. Targeting multidrug resistance in cancer. Nat Rev Drug Discov 2006;5:219-34.

23. Minchinton AI, Tannock IF. Drug penetration in solid tumours. Nat Rev Cancer 2006;6:583-92.

24. Hogdall D, Lewinska M, Andersen JB. Desmoplastic Tumor Microenvironment and Immunotherapy in Cholangiocarcinoma. Trends Cancer 2018;4:239-55.

25. Sherman MH, Yu RT, Tseng TW, Sousa CM, Liu S, Truitt ML, et al. Stromal cues regulate the pancreatic cancer epigenome and metabolome. Proc Natl Acad Sci U S A 2017;114:1129-34.

26. Sousa CM, Biancur DE, Wang X, Halbrook CJ, Sherman MH, Zhang L, et al. Pancreatic stellate cells support tumour metabolism through autophagic alanine secretion. Nature 2016;536:479-83.

27. Chuaysri C, Thuwajit P, Paupairoj A, Chau-In S, Suthiphongchai T, Thuwajit C. Alpha-smooth muscle actin-positive fibroblasts promote biliary cell proliferation and correlate with poor survival in cholangiocarcinoma. Oncol Rep 2009;21:957-69.

28. Okabe H, Beppu T, Hayashi H, Horino K, Masuda T, Komori H, et al. Hepatic stellate cells may relate to progression of intrahepatic cholangiocarcinoma. Ann Surg Oncol 2009;16:2555-64.

29. Watt J, Kocher HM. The desmoplastic stroma of pancreatic cancer is a barrier to immune cell infiltration. Oncoimmunology 2013;2:e26788.

30. Radhakrishnan VM, Kojs P, Young G, Ramalingam R, Jagadish B, Mash EA, et al. pTyr421 cortactin is overexpressed in colon cancer and is dephosphorylated by curcumin: involvement of non-receptor type 1 protein tyrosine phosphatase (PTPN1). PLoS One 2014;9:e85796.

31. Zhang X, Liu K, Zhang T, Wang Z, Qin X, Jing X, et al. Cortactin promotes colorectal cancer cell proliferation by activating the EGFR-MAPK pathway. Oncotarget 2017;8:1541-54.

32. Patel AS, Schechter GL, Wasilenko WJ, Somers KD. Overexpression of EMS1/cortactin in NIH3T3 fibroblasts causes increased cell motility and invasion in vitro. Oncogene 1998;16:3227-32.

ABSTRACT (IN KOREAN)

담도암에서 예후인자로서 Cortactin의 중요성 및 치료 타겟 물질로서의 관련 신호 전달체계

<지도교수 이 익 재>

연세대학교 대학원 의학과

조 연 아

목적: 담도암 높은 사망률을 보이는 예후가 좋지 않은 암종이나, 아직까지는 선택할 수 있는 치료가 제한적이며, 예후 예측을 위한 독립적인 요소는 부족하다. Cortactin (CTTN)은 다양한 종류의 암에서 세포 운동성 및 침윤과 연관이 있다고 알려져 있다. 본 연구에서는, 담도암에서 세포 및 동물실험 모델을 통하여 CTTN 발현 여부에 따른 담도암의 특성을 살펴보고, 예후 인자로서 역할을 탐구하였다. 또한 담도암 환자에서 CTTN 발현과 임상적 요인 및 예후와의 관계를 조사 하였다.

대상 및 방법: 우리는 KKU-M213 담도암 세포주를 사용하여 CTTN과 tyrosine466 인산화-CTTN (pY466-CTTN)이 모두 억제된 세포주를 확립하였다. Cancer-associated fibroblast (CAF)는 담관암 환자로부터 얻었다. Orthotopic 모델의 경우, 종양 세포 ($1x10^7$)를 6-8 주령 암컷 누드 마우스의 오른쪽 간에 주입하였다. 환자 분석을 위해서는 2005 년부터 2013 년 사이에 수술을 받은 담도암 환자 116 명의 임상 정보와 조직을 활용하였고, 이 환자들의 Tissue microarray를 구축하였다. 환자들은 pY466-CTTN의 발현정도에 따라 두 그룹으로 나누어 분석하였다: Hitoscore 0-100 (CTTN low) vs. 101-300 (CTTN hign).

결과: CTTN의 억제는 KKU-M213 세포주에서 침입과 이동성을 감

소시켰다. 또한 CTTN 억제 세포주와 CAF를 함께 함께 배양했을 때 CAF의 침입과 증식이 현저하게 감소하였다. CXCL10 및 CCL2의 mRNA 발현은 scrambled clone에 비해 CTTN 억제 세포에서 현저하게 감소했으며, 이러한 사이토카인은 CAF의 침입 및 증식에 영향을 미쳤다. Western blot 분석에서 MAPK 신호전달체계 물질인, p38, MEK 및 ERK의 인산화도 CTTN 억제 세포에서 감소됨을 보였다. 총 EGFR의 농도는 CTTN 억제 세포에서 EGF 자극을 하였을 때 지속적으로 감소하였으나, scrambled control 에서는 EGF에 자극에 의한 EGFR의 감소는 거의 보이지 않았다. 이종 이식 모델에서 CTTN 발현은 종양 주변의 섬유화와 상당한 연관성을 보였다. 환자분석에서도, pY466-CTTN (n = 64) 발현이 더 높은 환자는 안좋은 무병 생존율 (DFS) 및 전체 생존율 (OS)을 보였다 (Median DFS 7 vs. 16 개월, p <0.001; 및 median OS 19 vs . 53 개월, p <0.001). Cox- 회귀 다변량 분석에서는 높은 pY466-CTTN 발현이 DFS (HR, 2.33; 95 % CI 1.52-3.57, p <0.001) 및 OS (HR 2.87, 95 % CI 1.78-4.61, p<0.001)에 대한 중요한 예후 인자로도 확인되었다. 종양 주변의 결합조직형성 반응과 CAF 의 침윤 또한 CTTN 이 높게 발현된 환자군에서 좀 더 빈번하였다.

결론 : 우리의 결과는 CTTN이 CAF의 침입 및 증식을 강화함으로써 desmoplastic reaction과 유의하게 연관되어 있음을 보여 주었다. 또한 pY466-CTTN의 발현이 높은 환자는 DFS 및 OS가 더 나쁘고 종양 주변의 desmoplastic reaction이 증가하였다. CTTN에 의해 강화 된 EGFR-MAPK 신호전달체계가 이 것과 연관이 있을 것으로 생각된다.

핵심되는 말 : CTTN, cortactin, 담도암, 암관련섬유아세포, 결합조직형성, 섬유화